Correlation Between Seismic Intensity Measures and Response of Skewed Bridges

Van-Tien Phan and Duy-Duan Nguyen

1 Introduction

In seismic design codes and structural analysis procedures, they have commonly used the peak ground acceleration (PGA) or spectral acceleration (S_a) as the seismic IMs. However, many studies demonstrated that PGA or S_a are not the best selections for the seismic design and damage analyses of both on-ground and underground structures [1–9].

The interrelations between seismic IMs and seismic responses of reinforce concrete (RC) buildings were numerously studied [1, 2, 5, 7, 10–15]. Moreover, the correlation between seismic motion parameters and damage of other civil engineering structures such as tunnels [3, 16], storage tanks [17], nuclear power plants [18], and chimneys [19] were studied thoroughly. Numerous studies were performed to identify the good IMs for seismic damages of bridges. Padgett et al. [20] evaluated optimal IMs for deriving seismic fragility analysis models of multi-span steel girder bridges. Considering artificial and recorded earthquake motions, they concluded that PGA and $S_a(T_1)$ are efficient intensity measures for the artificial ground motions, while cumulative absolute velocity (CAV) is the most reliable for using recorded motions. Zhang et al. [9] identified the correlation between seismic IMs of far-field motions and the structural response of a cable-stayed bridge with a single pylon in China. The best correlated IMs exhibited were velocity spectral intensity (VSI), $S_a(T_1)$, and Housner intensity (HI). Jahangiri et al. [21] pointed out that root-mean-square of acceleration (A_{rms}) is the optimal intensity measure for seismic performance assessment of concrete arch bridges. In the study of Zelaschi et al. [22], by investigating a set of Italian RC bridges with 30 scaled motions they pointed out that Fajfar intensity (I_v), peak ground velocity (PGV), and S_a are the optimal IMs. Avşar

V.-T. Phan · D.-D. Nguyen (✉)
Department of Civil Engineering, Vinh University, Vinh, Vietnam
e-mail: duyduankxd@vinhuni.edu.vn

S. Kolathayar and S. C. Chian (eds.), *Recent Advances in Earthquake Engineering*,
Lecture Notes in Civil Engineering 175,
https://doi.org/10.1007/978-981-16-4617-1_3

et al. [23] highlighted that accelerated-related IMs are not strongly correlated with the response of seismic-isolated bridges. Additionally, the period-dependent IMs (e.g., VSI, HI, modified acceleration spectrum intensity, and S_a) are strongly correlated with the deformation base-isolated bridges subjected to normal earthquakes. Meanwhile, PGV and modified velocity spectrum intensity are good correlation for pulse-like ground motions.

Previously, the correlation between seismic IMs and damage of buildings and conventional bridges were well-studied, but it is still insufficient for skewed bridges. Specifically, the influence of earthquake frequency contents on the correlation analyses was not considered yet. This study aims to sufficiently recognize the relation between 23 ground motion IMs and seismic performances of skewed bridges accounting for the low- and high-frequency contents of earthquake. Accordingly, the strong and weak correlation IMs with structural performances of bridges also identified based on correlation analyses.

2 Seismic Intensity Measures and Ground Motions

To obtain the seismic IMs, a direct evaluation from earthquake accelerograms and a calculation by the software can be implemented [24]. This study accounts for 23 common ground motion IMs for correlation analyses. These parameters are calculated for every motion record using SeismoSignal software [25]. The considered IMs and its definitions are presented in Table 1.

Some undefined notations in Table 1 can be expressed as t_{tot} which is the total duration of earthquake; $a(t)$, $v(t)$, and $d(t)$ are the time-history acceleration, velocity, and displacement of the record; g is the gravity acceleration; ξ is the damping ratio; S_a is the spectral acceleration; PS_v is the pseudo-spectral velocity; T is the period; T_1 is the fundamental period; C_i is the Fourier factor; and f_i is the discrete frequency.

We selected 290 acceleration records from historic earthquakes. The data is available in PEER center [36] and KMA [37]. The magnitude of the earthquakes is ranged from 3.0 to 7.6. Low- and high-frequency content motions are divided with 212 records falling to the low-frequency set and 78 records belonging to the high-frequency set. It is important to note that the ground motion frequency content is normally recognized from the response spectra. The earthquake motions with large spectral accelerations fallen in the frequency range approximately larger than 10 Hz is considered as a high-frequency (HF) ground motion, otherwise discerned as low-frequency (LF) motions [38, 39]. Figure 1 shows the response spectra of two groups of ground motion records.

Table 1 Selected earthquake IMs

No.	Seismic IMs	Definition	Unit	Refs.
1	Peak ground acceleration	PGA = max |a(t)|	g	–
2	Peak ground velocity	PGV = max |v(t)|	m/s	–
3	Peak ground displacement	PGD = max |d(t)|	m	–
4	Ratio of PGV/PGA	PGV/PGA	s	[24]
5	Root-mean-square of acceleration	$A_{rms} = \sqrt{\frac{1}{t_{tot}} \int_0^{t_{tot}} a(t)^2 dt}$	g	[26]
6	Root-mean-square of velocity	$V_{rms} = \sqrt{\frac{1}{t_{tot}} \int_0^{t_{tot}} v(t)^2 dt}$	m/s	[24]
7	Root-mean-square of displacement	$D_{rms} = \sqrt{\frac{1}{t_{tot}} \int_0^{t_{tot}} d(t)^2 dt}$	m	[24]
8	Arias intensity	$I_a = \frac{\pi}{2g} \int_0^{t_{tot}} a(t)^2 dt$	m/s	[27]
9	Characteristic intensity	$I_c = (A_{rms})^{2/3} \sqrt{t_{tot}}$	$m^{1.5}/s^{2.5}$	[28]
10	Specific energy density	$\text{SED} = \int_0^{t_{tot}} v(t)^2 dt$	m^2/s	–
11	Cumulative absolute velocity	$\text{CAV} = \int_0^{t_{tot}} \|a(t)\| dt$	m/s	[29]
12	Acceleration spectrum intensity	$\text{ASI} = \int_{0.1}^{0.5} S_a(\xi = 0.05, T) dT$	g*s	[30]
13	Velocity spectrum intensity	$\text{VSI} = \int_{0.1}^{2.5} S_v(\xi = 0.05, T) dT$	m	[31]
14	Housner spectrum intensity	$\text{HI} = \int_{0.1}^{2.5} PS_v(\xi = 0.05, T) dT$	m	[30]
15	Sustained maximum acceleration	SMA = the 3rd of PGA	g	[32]
16	Sustained maximum velocity	SMV = the 3rd of PGV	m/s	[32]
17	Effective peak acceleration	$\text{EPA} = \frac{mean(S_a^{0.1-0.5}(\xi=0.05))}{2.5}$	g	[29]
18	Spectral acceleration at T_1	$S_a(T_1)$	g	[33]
19	Spectral velocity at T_1	$S_v(T_1)$	m/s	–
20	Spectral displacement at T_1	$S_d(T_1)$	m	–
21	A95 parameter	$A_{95} = 0.764\, I_a^{0.438}$	g	[34]
22	Predominant period	T_p	s	[24]
23	Mean period	$T_m = \frac{C_i^2/f_i)}{C_i^2}$	s	[35]

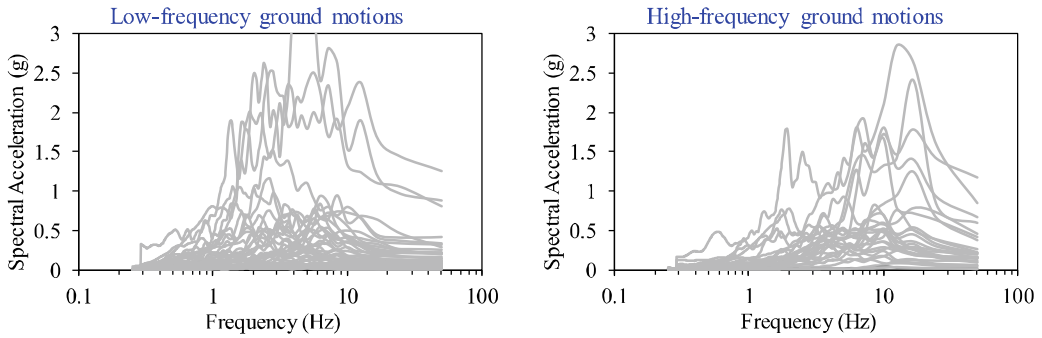

Fig. 1 Response spectra of selected ground motion records

3 Bridge Modelling

The studied bridge is made of reinforced concrete (RC) with 10 triple-column bents. The circular cross-section of all piers has a diameter of 0.8 m. The bridge has 11 spans, and each span is 14.5 m length. The column height of bent P1 and P2 is 4.0 m, while that for bent P4–P6 is 6.0 m, and for other bents is 5.5 m. The bridge is skewed with an angle of 60°. The configuration and dimensions of the bridge are also shown in Fig. 2. For the foundation of bridge bents, 12 bored piles (D = 0.4 m) arranged in a double-row are connected with the pile-cap which its dimensions in the height, width, and length are 0.9 m, 2.5 m, and 10 m, respectively. The length of piles is

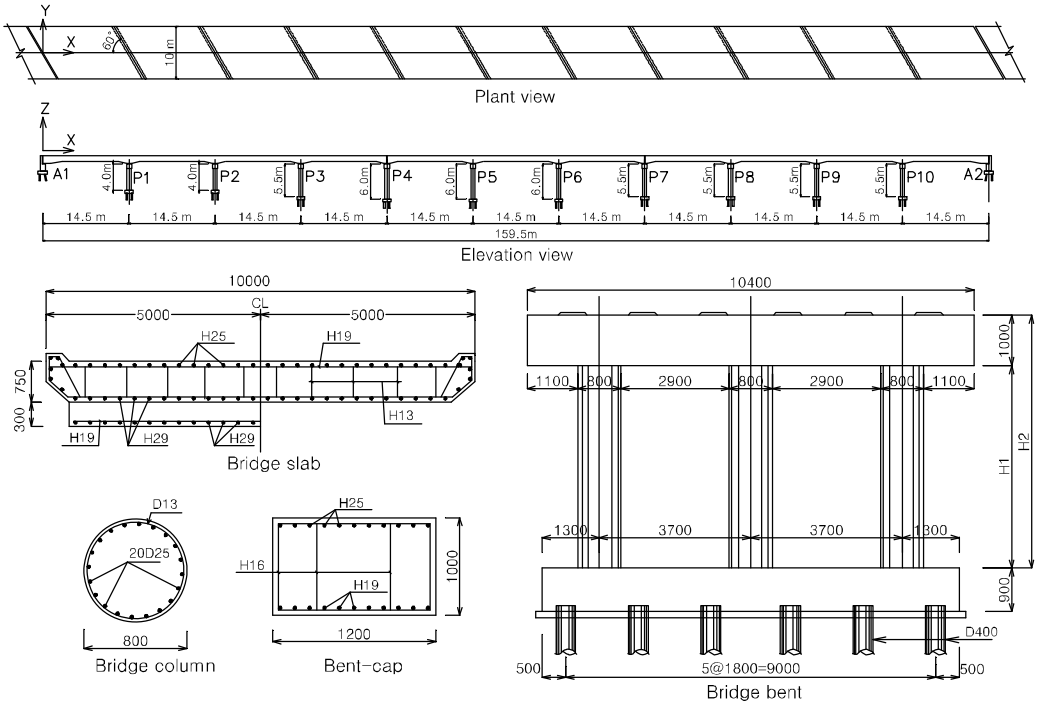

Fig. 2 Configurations of the RC skewed bridges

reduced from 22 m (at the bent P1) to 10 m (at the bent P10). The piles are mostly embedded into sand, gravel-sand, amber gravel, weathered rock and soft rock layers.

The open-source platform, OpenSees [40], is employed to build the finite element model of the bridge. To model concrete material, the *concrete02* model is used [41], whereas the *steel02* model is applied for modelling reinforcement in OpenSees [42]. It is noted that those models are able to consider the nonlinearity of materials [43–47].

The girder of bridges is assumed to be elastic behaviour during seismic excitations. Thus, the *ElasticMembranePlateSection* element is assigned to the bridge slab. The column bridge is modelled using *nonlinearBeamColumn* elements. Figure 3 shows the fiber-section modelling scheme of the bridge column. Also, the moment–curvature relation of column cross-sections are presented in Fig. 3. Additionally, considering the soil-structure interaction in the bridge, the piles are modelled using elastic beam elements, in which a series of soil springs are attached to element nodes. To model soil springs, the *zerolength* model represented by *p-y* curve [48] is utilized, as illustrated in Fig. 4. Figure 5 shows the 3D finite element modelling of the bridges in OpenSees. The eigenvalue analysis result is described in Fig. 6.

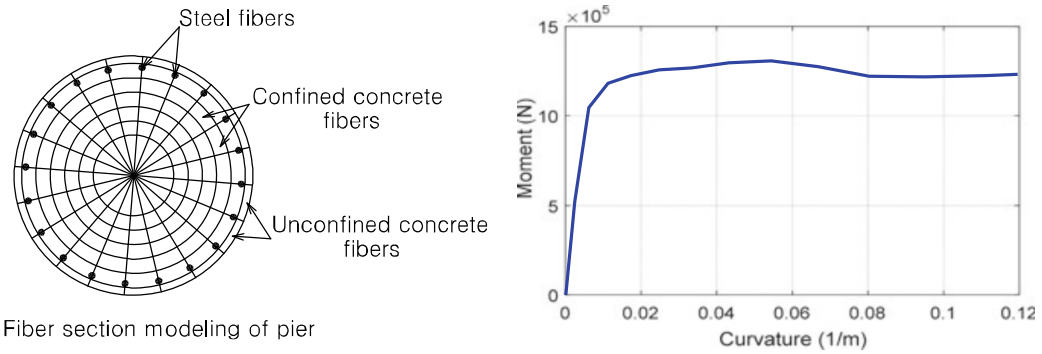

Fig. 3 Fiber section model and moment–curvature relationship of the bridge piers

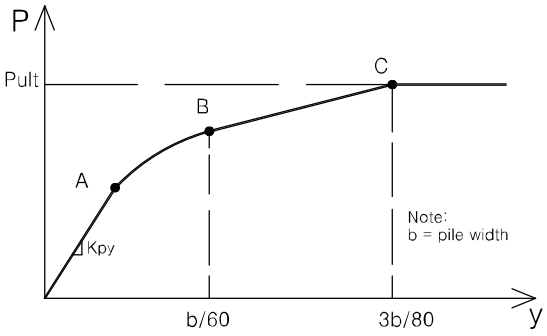

Fig. 4 Illustration of the *p-y* curve for soil-pile interaction modeling

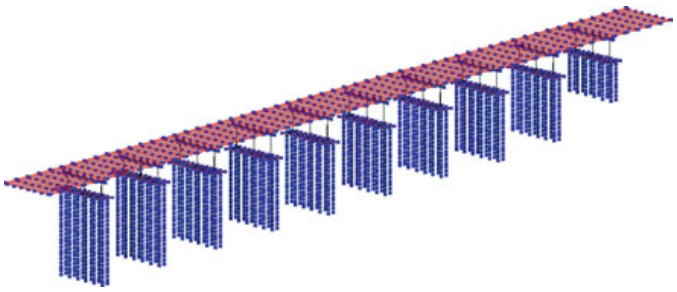

Fig. 5 3D finite element model of the bridge in OpenSees

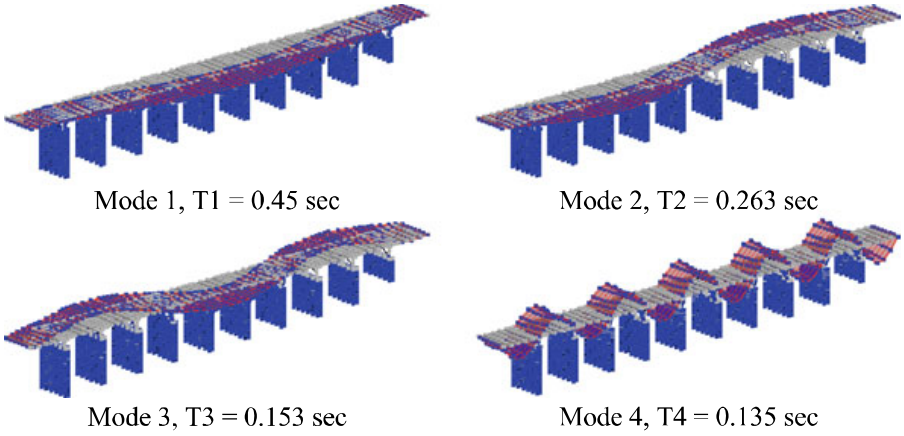

Fig. 6 Eigenvalue analysis results

4 Seismic Response and Correlation Analysis

A series of nonlinear time-history analyses were performed. We imposed all ground motions in two groups on the bridge model in horizontal directions and captured the structural responses associated with each ground motion. Since the pier is one of the most crucial components of the bridge structures, seismic performances of the bridge are measured in terms of the drift ratio and shear forces of bridge piers. The use of displacement (or drift ratio) and internal forces is common and facilitated in the seismic design and fragility analyses [43–47, 49]. Figure 7 illustrates responses of the bridge subjected to the 1989 Loma Prieta and the 2016 Gyeongju earthquake, in which the displacement is measured at the top of the middle pier, while the shear force is monitored at the bottom of that pier. The responses of all bridge piers are obtained for every ground motion records.

The relationship between seismic responses of the structure and earthquake IMs is needed to identify the strong and the weak correlation indicators. For this study, the Pearson's coefficient is used to reflect the correlation between seismic responses of the bridge and earthquake IMs. The linear correlation coefficient given in Ang and Tang [50] is defined as

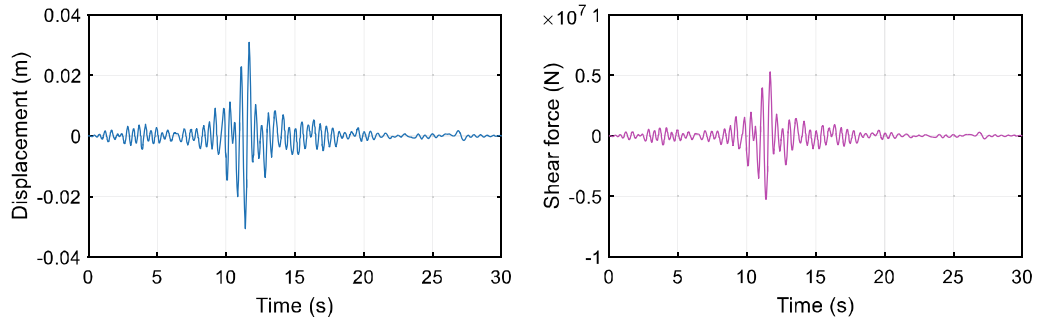

(a) Seismic responses of bridge under the 1989 Loma Prieta (LF) earthquake

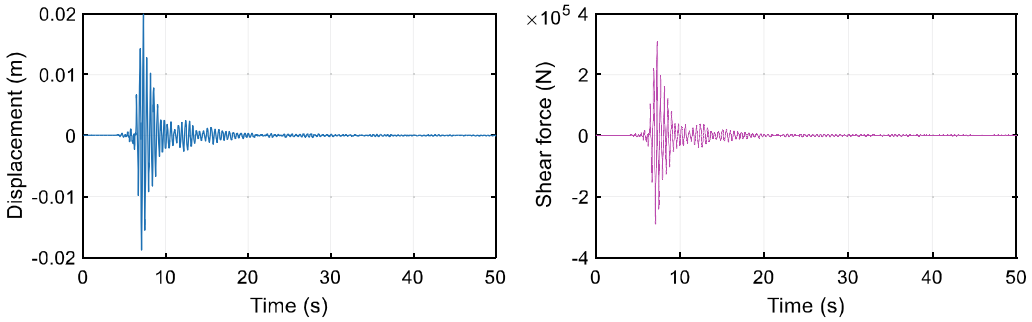

(b) Seismic responses of bridge under the 2016 Gyeongju (HF) earthquake

Fig. 7 Example of seismic responses of the bridge under LF and HF earthquakes

$$\rho = \frac{1}{n-1}\frac{\sum(x_i - \overline{x})(y_i - \overline{y})}{\sigma_x \sigma_y} \tag{1}$$

where $\overline{x}$, $\overline{y}$, are the sample means of variables x_i and y_i, and x_i represents the seismic responses of bridges, while y_i represents the intensity measures. σ_x,σ_y are the sample standard deviations of x and y, determined by

$$\sigma_x = \sqrt{\frac{1}{n-1}\left[(\Sigma x_i)^2 - n(\overline{x})^2\right]};\ \sigma_y = \sqrt{\frac{1}{n-1}\left[(\Sigma y_i)^2 - n(\overline{y})^2\right]} \tag{2}$$

We calculated the correlation coefficients for seismic responses of the bridge and IMs associated with two groups of ground motions. It should be noted that the results are showed here for a representative bridge pier because within a specific bridge the same trend is observed for all piers. Figures 8 and 9 show the calculated correlation coefficients corresponding to each earthquake IM for both LF and HF motions. In the case of low-frequency ground motions, it can be demonstrated that Arias intensity (I_a) has the strongest correlation with seismic damage, followed by characteristic intensity (I_c), $S_a(T_1)$, and spectral velocity at the fundamental period ($S_v(T_1)$). Whereas, PGV/PGA ratio, mean period (T_m), and predominant period (T_p) are weak correlated parameters with seismic damage of bridges. For the high-frequency ground motions, the strongest correlated measure with damage is specific energy density

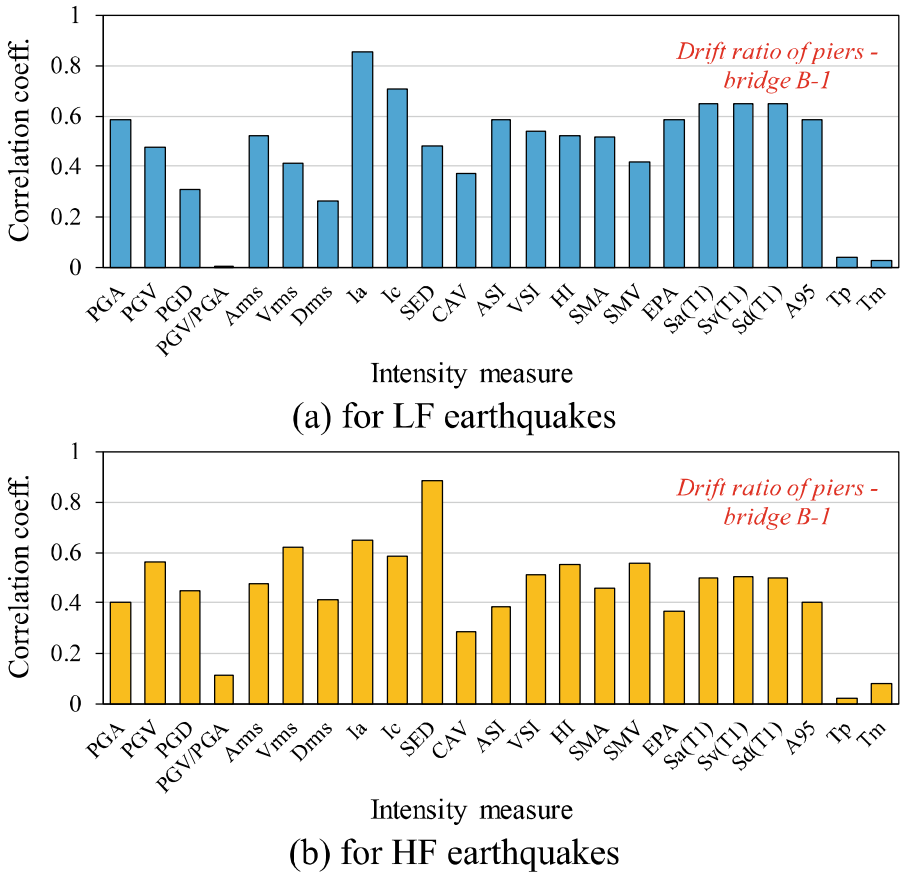

Fig. 8 Correlation between the dift ratio of piers and seismic IMs

(SED), followed by I_a, root-mean-square of velocity (V_{rms}) and I_c. Similar to the low frequency motion group, three low-correlated IMs are PGV/PGA ratio, T_m, and T_p. The results also indicate that PGA and PGV have medium correlation and it may not always the best parameters for seismic design and seismic vulnerability assessment of skewed bridges.

This study identified the strongly correlated earthquake IMs for seismic responses of skewed RC bridges. Designers or analysts can use $S_a(T_1)$, $S_v(T_1)$, I_a or I_c for the design or performance evaluation process as well as fragility analyses of such bridges. Also, the findings of this paper imply that we should not use PGV/PGA, T_m or T_p for seismic design and analyses of the bridges. These findings are partially consistent with those of Padgett et al. [20] and Jahangiri et al. [21] since the bridge type is not similar.

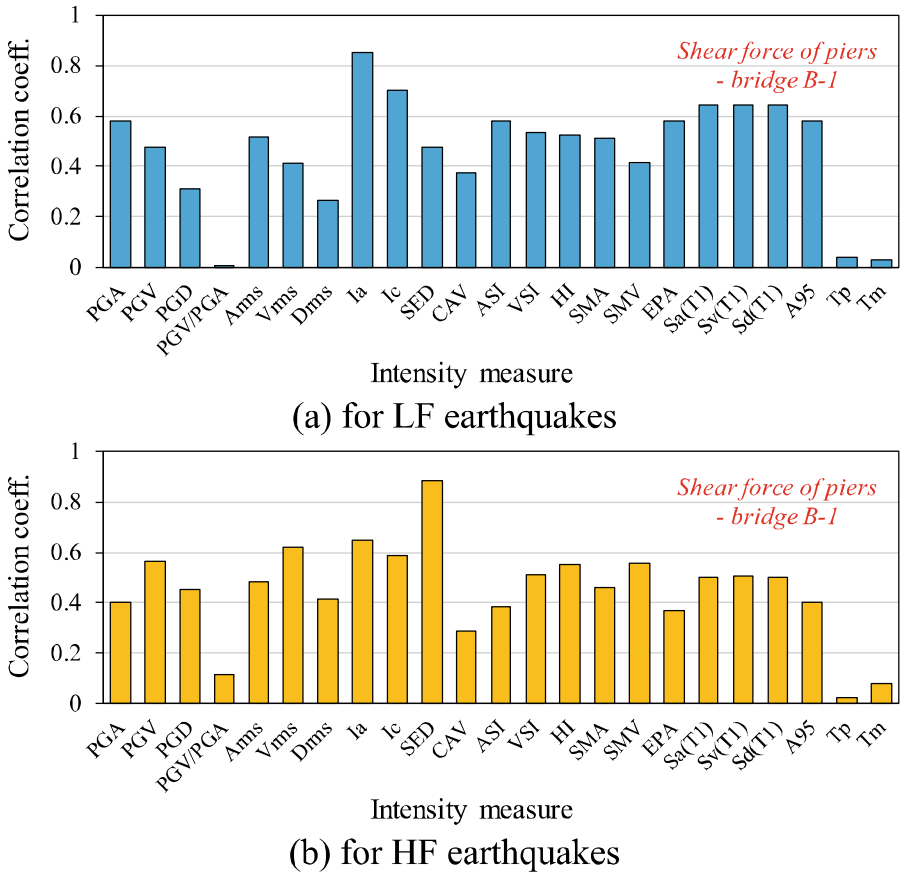

Fig. 9 Correlation between the shear force of piers and seismic IMs

5 Conclusions

A series of nonlinear time-history analyses are performed for the skewed bridge. Two groups of earthquake ground motions classified into low- and high-frequency contents are used for analyses. For each ground motion, 23 seismic intensity measures are considered. A series of correlation coefficients between seismic responses of bridges and earthquake intensity measures are calculated. The following conclusions are drawn based on the analysis results.

- For the low frequency ground motions, the best intensity measure for correlating with seismic responses of bridges I_a, followed by I_c, $S_a(T_1)$, and $S_v(T_1)$.
- For the high frequency ground motions, the well-correlated IMs with seismic performances are SED, I_a, V_{rms}, and I_c.
- PGV/PGA, T_m, and T_p show to be weak correlated measures if bridges subjected to low frequency motions. This trend is also observed for the case of high frequency motions.
- PGA and PGV have a medium correlation with responses of bridge structures during both low- and high-frequency earthquake motions. A selection of PGA or

PGV for seismic design and seismic vulnerability assessment of bridges may not be the best option.

References

1. Cao V, Ronagh H (2014) Correlation between seismic parameters of far-fault motions and damage indices of low-rise reinforced concrete frames. Soil Dyn Earthq Eng 66:102–112
2. Cao V, Ronagh H (2014) Correlation between parameters of pulse-type motions and damage of low-rise RC frames. Earthq Struct 7(3):365–384
3. Chen Z, Wei J (2013) Correlation between ground motion parameters and lining damage indices for mountain tunnels. Nat Hazards 65(3):1683–1702
4. Corigliano M, Lai CG, Barla G (2007) Seismic vulnerability of rock tunnels using fragility curves. In: 11th ISRM congress. International Society for Rock Mechanics
5. Elenas A, Meskouris K (2001) Correlation study between seismic acceleration parameters and damage indices of structures. Eng Struct 23(6):698–704
6. Ghayoomi M, Dashti S (2015) Effect of ground motion characteristics on seismic soil-foundation-structure interaction. Earthq Spectra 31(3):1789–1812
7. Massumi A, Gholami F (2016) The influence of seismic intensity parameters on structural damage of RC buildings using principal components analysis. Appl Math Model 40(3):2161–2176
8. Yaghmaei-Sabegh S (2012) Application of wavelet transforms on characterization of inelastic displacement ratio spectra for pulse-like ground motions. J Earthq Eng 16(4):561–578
9. Zhang Y, Ding Y, Pang Y (2015) Selection of optimal intensity measures in seismic damage analysis of cable-stayed bridges subjected to far-fault ground motions. J Earthq Tsunami 9(01):1550003
10. Elenas A (2000) Correlation between seismic acceleration parameters and overall structural damage indices of buildings. Soil Dyn Earthq Eng 20(1–4):93–100
11. Nanos N, Elenas A, Ponterosso P (2008) Correlation of different strong motion duration parameters and damage indicators of reinforced concrete structures. In: The 14th word conference on earthquake engineering, Beijing, China
12. Kostinakis K, Athanatopoulou A, Morfidis K (2015) Correlation between ground motion intensity measures and seismic damage of 3D R/C buildings. Eng Struct 82:151–167
13. Pejovic J, Jankovic S (2015) Selection of ground motion intensity measure for reinforced concrete structure. Procedia Eng 117:588–595
14. Pejovic J, Serdar N, Pejovic R (2017) Optimal intensity measures for probabilistic seismic demand models of RC high-rise buildings. Earthq Struct 13(3):221–230
15. Lu X, Ye L, Lu X, Li M, Ma X (2013) An improved ground motion intensity measure for super high-rise buildings. Science China Technol Sci 56(6):1525–1533
16. Nguyen DD, Park D, Shamsher S, Nguyen VQ, Lee TH (2019) Seismic vulnerability assessment of rectangular cut-and-cover subway tunnels. Tunn Undergr Space Technol 86:247–261
17. Phan HN, Paolacci F (2016) Efficient intensity measures for probabilistic seismic response analysis of anchored above-ground liquid steel storage tanks. In: Pressure vessels and piping conference. American Society of Mechanical Engineers
18. Nguyen DD, Thusa B, Han TS, Lee TH (2020) Identifying significant earthquake intensity measures for evaluating seismic damage and fragility of nuclear power plant structures. Nucl Eng Technol 52(1):192–205
19. Qiu Y, Zhou C, Siha A (2020) Correlation between earthquake intensity parameters and damage indices of high-rise RC chimneys. Soil Dyn Earthq Eng 137:106282
20. Padgett JE, Nielson BG, DesRoches R (2008) Selection of optimal intensity measures in probabilistic seismic demand models of highway bridge portfolios. Earthq Eng Struct Dynam 37(5):711–725

21. Jahangiri V, Yazdani M, Marefat MS (2018) Intensity measures for the seismic response assessment of plain concrete arch bridges. Bull Earthq Eng 16(9):4225–4248
22. Zelaschi C, Monteiro R, Pinho R (2019) Critical assessment of intensity measures for seismic response of Italian RC bridge portfolios. J Earthq Eng 23(6):980–1000
23. Avşar Ö, Özdemir G (2011) Response of seismic-isolated bridges in relation to intensity measures of ordinary and pulselike ground motions. J Bridg Eng 18(3):250–260
24. Kramer SL (1996) Geotechnical earthquake engineering. Prentice Hall, Inc., Upper Saddle River, New Jersey, USA
25. SeismoSignal (2020) A computer program for signal processing of strong-motion data. http://www.seismosoft.com. Accessed June
26. Dobry R, Idriss IM, Ng E (1978) Duration characteristics of horizontal components of strong-motion earthquake records. Bull Seismol Soc Am 68(5):1487–1520
27. Arias A (1970) A measure of earthquake intensity. Massachusetts Inst of Tech, Cambridge. Univ of Chile, Santiago de Chile
28. Park Y, Ang AH, Wen YK (1985) Seismic damage analysis of reinforced concrete buildings. J Struct Eng 111(4):740–757
29. Benjamin JR (1988) A criterion for determining exceedance of the operating basis earthquake. Report EPRI NP-5930, Electrical Power Research Institute, Palo Alto, California
30. Housner GW (1952) Spectrum intensities of strong-motion earthquakes. In: Symposium on earthquake and blast effects on structures, Los Angeles, California, USA, pp 20–36
31. Thun JL (1988) Earthquake ground motions for design and analysis of dams. In: Earthquake engineering and soil dynamics II-recent advances in ground-motion evaluation
32. Nuttli OW (1979) The relation of sustained maximum ground acceleration and velocity to earthquake intensity and magnitude. Report 16, Misc. Paper S-73-1, US Army Waterways Experimental Station, Vicksburg, Mississippi
33. Shome N, Cornell CA, Bazzurro P, Carballo JE (1998) Earthquakes, records, and nonlinear responses. Earthq Spectra 14(3):469–500
34. Sarma SK, Yang KS (1987) An evaluation of strong motion records and a new parameter A95. Earthq Eng Struct Dyna 15(1):119–132
35. Rathje EM, Norman AA, Bray J (1998) Simplified frequency content estimates of earthquake ground motions. J Geotech Geoenviron Eng 124(2)
36. PEER (2019) Pacific Earthquake Engineering Research Center Database, http://peer.berkeley.edu/peer_ground_motion_database
37. KMA (2019) Korean Meteorological Administration, Korea
38. EPRI (2007) Program on technology innovation: the effects of high frequency ground motion on structures, components, and equipment in nuclear power plants. Report 1015108, Electrical Power Research Institute, Palo Alto, California, USA
39. EPRI (2017) Advanced nuclear technology: high-frequency seismic loading evaluation for standard nuclear power plants. Report 3002009429, Electrical Power Research Institute, Palo Alto, California, USA
40. Mazzoni S, McKenna F, Fenves GL (2005) OpenSees command language manual. Pacific Earthquake Engineering Research (PEER) Center
41. Kent DC, Park R (1971) Flexural members with confined concrete. J Struct Division
42. Menengotto M (1973) Method of analysis for cyclically loaded reinforced concrete plane frames including changes in geometry and nonelastic behavior of elements under combined normal force and bending. In: IABSE symposium on resistance and ultimate deformability of structures acted on by well-defined repeated loads, Lisbon
43. Lee TH, Nguyen DD (2018) Seismic vulnerability assessment of a continuous steel box girder bridge considering influence of LRB properties. Sādhanā 43(1):14
44. Nguyen DD, Lee TH (2018) Seismic fragility curves of bridge piers accounting for ground motions in Korea. IOP Conf Ser Earth Environ Sci 143(1):012029
45. Tran NL, Nguyen TH, Phan VT, Nguyen DD (2020) Seismic fragility analysis of reinforced concrete piers of steel box girder bridges: a parametric study. Mater Today Proc

46. Lee TH, Nguyen VH, Phan VT, Nguyen DD (2018) Seismic margin assessment of a reinforced concrete skewed bridge in a nuclear power plant. MATEC Web of Conferences 251:02019
47. Choi BH, Moreno LB, Lim CS, Nguyen DD Lee TH (2019) Seismic performance evaluation of a fully integral concrete bridge with end-restraining abutments. Adv Civil Eng 2019
48. Reese LC, Cox WR, Koop F D (1974) Field testing and analysis of laterally loaded piles in sand. In: The VI annual offshore technology conference, Houston, Texas, pp 473–485
49. Park HS, Nguyen DD, Lee TH (2016) Seismic fragilities of bridges and transmission towers considering recorded ground motions in South Korea. J Earthquake Eng Soc Korea 20(7_spc):435–441
50. Ang AH, Tang WH (2007) Probability concepts in engineering: emphasis on applications in civil & environmental engineering, vol 1. Wiley, New York